Bioorganic Chemistry 87 (2019) 585–593

Contents lists available at ScienceDirect

Bioorganic Chemistry

journal homepage: www.elsevier.com/locate/bioorg

Withanolides from *Physalis peruviana* showing nitric oxide inhibitory effects and affinities with iNOS

Bangjian Dong[a], Lijun An[a], Xueyuan Yang[a], Xuke Zhang[a], Jie Zhang[b], Muhetaer Tuerhong[c], Da-Qing Jin[d], Yasushi Ohizumi[e], Dongho Lee[f], Jing Xu[a,*], Yuanqiang Guo[a,*]

[a] State Key Laboratory of Medicinal Chemical Biology, College of Pharmacy, and Tianjin Key Laboratory of Molecular Drug Research, Nankai University, Tianjin 300050, People's Republic of China
[b] Key Laboratory for Green Processing of Chemical Engineering of Xinjiang Bingtuan, School of Chemistry and Chemical Engineering, Shihezi University, Shihezi 832003, People's Republic of China
[c] College of Chemistry and Environmental Sciences, Laboratory of Xinjiang Native Medicinal and Edible Plant Resources Chemistry, Kashgar University, Kashgar 844000, People's Republic of China
[d] School of Medicine, Nankai University, Tianjin 300071, People's Republic of China
[e] Department of Medical Biochemistry, School of Pharmaceutical Sciences, University of Shizuoka, Shizuoka 422-8526, Japan
[f] Department of Biosystems and Biotechnology, College of Life Sciences and Biotechnology, Korea University, Seoul 136-713, Republic of Korea

ARTICLE INFO

Keywords:
Physalis peruviana
Withanolides
NO inhibitors
Molecular docking
iNOS

ABSTRACT

A phytochemical study to obtain new nitric oxide (NO) inhibitors resulted in the isolation of five new withanolides from the whole plants of *Physalis peruviana*. The structures were determined on the basis of extensive NMR spectroscopic data analysis as well as the time-dependent density functional theory (TDDFT) electronic circular dichroism (ECD) calculations. The NO inhibitory effects were examined by inhibiting NO release in lipopolysaccharide-stimulated murine microglial BV-2 cells. Molecular docking studies showed the strong interactions of bioactive compounds with the inducible nitric oxide synthase (iNOS) protein, revealing the potential mechanism of NO inhibition of bioactive compounds.

1. Introduction

Nitric oxide (NO) is a physiological messenger molecule involving in many physiological functions, such as regulation of neurotransmitter release and mediation of synaptic plasticity in central nervous system (CNS) [1–3]. In addition to the positive physiological roles, growing evidence suggested that high concentration of NO can cause the damage of DNA, RNA, lipids, etc. [4,5]. In CNS, excessive amount of NO contributes to microglia activation and neuroinflammatory responses, which has been proven to be neurotoxic and can cause neurodegeneration and chronic neurological disorders, such as Alzheimer's disease (AD), and Parkinson's disease (PD) [6–9]. Accumulating studies indicated NO to be a pivotal sign of inflammatory response, to inhibit excessive NO has become an effective strategy for inflammatory diseases and related neurodegenerative disorders [9–11].

Physalis peruviana L., belonging to the Solanaceae plant family, is a perennial herb cultivated mainly in southern China including Guangdong and Yunnan provinces [12]. Its fruit is a delicious source of healthy food and nutrition. In addition, the whole plant or its leaves have been used as a folk medicine for the treatment of fever, bronchitis, acute pyelonephritis, orchitis, and parotitis [13]. The major constituents of *P. peruviana* have been reported to be withanolides, which displayed diverse biological effects [14–23]. In our continuous search for new NO inhibitors as potential lead compounds for the treatment of inflammation and related neurodegenerative diseases, *P. peruviana* attracted our attention and its chemical constituents were investigated. Five new withanolides were isolated from the methanol extract of the whole plants of *P. peruviana*. Their structures were established on the basis of extensive NMR spectroscopic data analysis and the time-dependent density functional theory (TDDFT) electronic circular dichroism (ECD) calculations. The biological effects of NO inhibition and the interactions of bioactive compounds with the iNOS protein were also investigated. In this paper, the structural determination and NO inhibitory effects of these isolated withanolides as well as their interactions with the inducible nitric oxide synthase (iNOS) protein are described.

* Corresponding authors.
E-mail addresses: xujing611@nankai.edu.cn (J. Xu), victgyq@nankai.edu.cn (Y. Guo).

https://doi.org/10.1016/j.bioorg.2019.03.051
Received 27 December 2018; Received in revised form 22 February 2019; Accepted 18 March 2019
Available online 22 March 2019

2. Experimental

2.1. General experimental procedures

Optical rotations were recorded on an InsMark IP120 automatic polarimeter (InsMark Instrument Co., Ltd., Shanghai, People's Republic of China). ECD spectra were obtained on a JASCO J-715CD spectrometer (JASCO Corporation, Tokyo, Japan). Infrared (IR) spectra (film) were recorded on a Bruker Tensor 27 FT-IR spectrometer. 1D and 2D NMR experiments were performed on a Bruker AV 400 instrument (Bruker, Switzerland, 100 MHz for ^{13}C and 400 MHz for ^{1}H) with TMS as an internal reference at room temperature. ESIMS and HRESIMS were recorded by a Thermo Finnigan LCQ-Advantage mass spectrometer and an IonSpec 7.0 T FTICR MS (IonSpec Co., Ltd., Lake Forest, CA, USA), respectively. HPLC separations were conducted on a CXTH system, equipped with a Shodex RI-102 detector (Showa Denko Co., Ltd., Tokyo, Japan) and a YMC-pack ODS-AM (20 × 250 mm) column (YMC Co. Ltd., Kyoto, Japan). Silica gel (200–300 mesh) used for column chromatography was purchased from Qingdao Haiyang Chemical Group Co., Ltd. (Qingdao, People's Republic of China). Chemical reagents (analytical grade) and biological reagents were provided by Tianjin Chemical Reagent Co. (Tianjin, People's Republic of China) and Sigma Co., respectively. The BV-2 cell line was from Shanghai Institutes for Biological Sciences, Chinese Academy of Sciences (Shanghai, People's Republic of China).

2.2. Plant material

The whole plants of *P. peruviana* were collected from Jilin province, People's Republic of China, in August 2017. The botanical identification was made by one of the authors (Y. Guo), and a voucher specimen (No. 20170825DB) was deposited at the laboratory of the Research Department of Natural Medicine, College of Pharmacy, Nankai University.

2.3. Extraction and isolation

The air-dried whole plants of *P. peruviana* (10.0 kg) were extracted with MeOH (3 × 60 L) under reflux. The organic solvent was concentrated to afford a crude methanol extract (425.0 g) in vacuum. The resultant dark residue was dissolved in H_2O (0.5 L) and partitioned with EtOAc (5 × 0.5 L) to give EtOAc (225.0 g) fraction. Then the portion was subjected to a silica gel column chromatography (silica gel, 1300 g; column, 9 × 70 cm), using a gradient solvent system of petroleum ether-acetone (100: 0, 100: 2, 100: 4, 100: 7, 100: 10, 100: 14, 100: 19, 100: 27, and 100: 35, 20 L for each gradient elution), to afford eight fractions (F_1–F_8) based on TLC analysis. Fraction F_7 was separated by MPLC over octadecylsilane (ODS) eluting with a step gradient of 60–91% MeOH in H_2O to give four subfractions ($F_{7\text{-}1}$–$F_{7\text{-}4}$). Using preparative HPLC (YMC-pack ODS-AM, 20 × 250 mm, 77% MeOH in H_2O), compound **1** (t_R = 24 min, 8.3 mg) was obtained from $F_{7\text{-}3}$. Fraction $F_{7\text{-}2}$ was purified by HPLC (68% MeOH in H_2O) to yield **5** (t_R = 40 min, 18.3 mg). Fraction F_5, with the same procedure as for fraction F_7, gave four subfractions ($F_{5\text{-}1}$–$F_{5\text{-}4}$). The subsequent purification of $F_{5\text{-}2}$ by the above HPLC system (76% MeOH in H_2O) to afford compound **2** (t_R = 32 min, 6.9 mg). Using the same MPLC, fraction F_6 gave three subfractions ($F_{6\text{-}1}$–$F_{6\text{-}3}$). Compound **4** (t_R = 55 min, 16.8 mg) was isolated from $F_{6\text{-}2}$ (70% MeOH in H_2O). Through the same procedure as for F_6, seven subfractions ($F_{8\text{-}1}$–$F_{8\text{-}7}$) were obtained over MPLC (ODS column) from F_8. Fraction $F_{8\text{-}6}$ was purified via HPLC (80% MeOH in H_2O) to afford compound **3** (t_R = 60 min, 8.2 mg).

*Peruvianolide A (**1**):* amorphous powder; [α] − 4 (*c* 0.2, CH_2Cl_2); ECD (CH_3CN) 213 (Δε + 0.84) nm; IR (film) ν_{max} 3420, 2928, 2867, 1716, 1646, 1223, 735 cm^{-1}; ^{1}H NMR (400 MHz, $CDCl_3$) and ^{13}C NMR (100 MHz, $CDCl_3$) data, see Tables 1 and 2; ESIMS *m/z* 461 $[M + H]^+$; HRESIMS *m/z* 461.3270 $[M + H]^+$, calcd for $C_{28}H_{45}O_5$, 461.3267.

*Peruvianolide B (**2**):* colorless solid; [α] − 58.7 (*c* 0.1, CH_2Cl_2); ECD (CH_3CN) 221 (Δε + 3.59), 264 (Δε − 0.83), 281 (Δε − 0.24), 327 (Δε − 1.56) nm; IR (film) ν_{max} 3421, 2925, 1701, 1658, 1245, 1036, 734 cm^{-1}; ^{1}H NMR (400 MHz, $CDCl_3$) and ^{13}C NMR (100 MHz, $CDCl_3$) data, see Tables 1 and 2; ESIMS *m/z* 455 $[M + H]^+$; HRESIMS *m/z* 455.2800 $[M + H]^+$, calcd for $C_{28}H_{39}O_5$, 455.2797.

*Peruvianolide C (**3**):* amorphous powder; [α] − 41.9 (*c* 0.2, CH_2Cl_2); ECD (CH_3CN) 197 (Δε − 19.29), 215 (Δε + 7.03) nm; IR (film) ν_{max} 3446, 2953, 1730, 1677, 1246, 1106, 1055, 712 cm^{-1}; ^{1}H NMR (400 MHz, $CDCl_3$) and ^{13}C NMR (100 MHz, $CDCl_3$) data, see Tables 1 and 2; ESIMS *m/z* 545 $[M + H]^+$; HRESIMS *m/z* 545.3119 $[M + H]^+$, calcd for $C_{31}H_{45}O_8$, 545.3114.

*Peruvianolide D (**4**):* amorphous powder; [α] − 4.8 (*c* 0.2, CH_2Cl_2); ECD (CH_3CN) 214 (Δε + 3.92) nm; IR (film) ν_{max} 3447, 2929, 1717, 1670, 1239, 1136, 733 cm^{-1}; ^{1}H NMR (400 MHz, $CDCl_3$) and ^{13}C NMR (100 MHz, $CDCl_3$) data, see Tables 1 and 2; ESIMS *m/z* 473 $[M + H]^+$; HRESIMS *m/z* 473.2905 $[M + H]^+$, calcd for $C_{28}H_{41}O_6$, 473.2903.

*Peruvianolide E (**5**):* amorphous powder; [α] + 4.6 (*c* 0.5, CH_2Cl_2); ECD (CH_3CN) 242 (Δε − 0.03), 291 (Δε − 6.03) nm; IR (film) ν_{max} 3436, 2941, 1710, 1247, 1117, 953, 733 cm^{-1}; ^{1}H NMR (400 MHz, $CDCl_3$) and ^{13}C NMR (100 MHz, $CDCl_3$) data, see Tables 1 and 2; ESIMS *m/z* 585 $[M + Na]^+$; HRESIMS *m/z* 585.3037 $[M + Na]^+$, calcd for $C_{31}H_{46}NaO_9$, 585.3040.

2.4. Computational method

According to the conformation of every compound deduced from the NOESY spectrum and Chem3D modeling, the systematic conformational searches were performed firstly using MOE software, and then appropriate conformers were selected for geometry optimizations. Geometry optimizations and re-optimizations on the B3LYP/6-31 + G(d,p)level were performed by the Gaussian 09 package [24]. The TDDFT ECD calculations for the optimized conformers were carried out at the CAMB3LYP/SVP level with a CPCM solvent model in acetonitrile. The calculated ECD spectra of different conformers were simulated with a half bandwidth of ~0.4 eV. The ECD curves were extracted by SpecDis 1.62 software [25]. The overall ECD curves of all the compounds were weighted by Boltzmann distribution after UV correction.

2.5. MTT assay for cell viability

The cell viability was evaluated by the MTT experiment [26]. The BV-2 cells were seeded on 96-well plates with 3 × 10^4 cells per well in 100 μL culture medium. After 24 h, they were treated with various concentrations of test compounds for 24 h. The MTT (Sigma-Aldrich Co., St. Louis, Mo, USA) solution at the concentration of 5 mg/mL was added to the cells and incubated for 4 h at 37 °C. Then the medium was removed and dimethyl sulphoxide (DMSO; Sigma-Aldrich Co., St. Louis, Mo, USA) was added to each well to solubilize the formazan crystals in each cell. After 30 min incubation at 37 °C, the absorbance was measured at 492 nm using an automated microplate spectrophotometer (Thermo Fisher Scientific Inc., USA). Each experiment was repeated at least three times.

2.6. Bioassay for LPS-induced NO production in vitro

The evaluation of NO inhibitory effect was tested by inhibiting NO release in LPS-induced murine microglial BV-2 cells. The cells were cultured in DMEM with 10% (*v/v*) inactivated fetal bovine serum and 100 U/mL penicillin/streptomycin in a humidified incubator containing 95% air and 5% CO_2 at 37 °C. The cells were seeded into 96-wells culture plates at a density of 5 × 10^4 cells/well and allowed to adhere for 24 h at 37 °C. The cells were incubated for 20 h with or without 0.2 μg/mL of LPS (Sigma Chemical Co., St. Louis, MO, USA) in the absence or presence of the test compounds. 2-Methyl-2-thiopseudourea, sulfate (SMT) was used as a positive control. As a parameter of NO

Table 1
^{13}C NMR data for compounds **1–5** (δ in ppm, 100 MHz, in $CDCl_3$).[a]

Position	1		2		3		4		5	
1	72.9	CH	153.6	CH	202.4	C	203.7	C	209.8	C
2	38.2	CH_2	128.1	CH	132.1	CH	129.4	CH	39.5	CH_2
3	66.4	CH	185.4	C	142.0	CH	144.4	CH	77.5	CH
4	41.4	CH_2	125.0	CH	69.6	CH	33.0	CH_2	74.9	CH
5	137.3	C	161.5	C	63.6	C	62.0	C	64.8	C
6	125.6	CH	201.8	C	62.7	CH	63.3	CH	60.1	CH
7	31.8	CH_2	46.9	CH_2	30.4	CH_2	31.2	CH_2	30.5	CH_2
8	31.9	CH	49.0	CH	29.2	CH	29.9	CH	28.8	CH
9	41.6	CH	34.4	CH	43.8	CH	44.7	CH	42.4	CH
10	41.7	C	44.9	C	47.6	C	48.5	C	50.3	C
11	20.3	CH_2	22.8	CH_2	22.2	CH_2	23.6	CH_2	21.4	CH_2
12	39.5	CH_2	39.1	CH_2	39.5	CH_2	39.6	CH_2	39.3	CH_2
13	42.7	C	43.1	C	43.1	C	42.6	C	43.1	C
14	56.3	CH	55.9	CH	58.9	CH	55.9	CH	58.7	CH
15	24.4	CH_2	24.1	CH_2	76.0	CH	24.1	CH_2	76.2	CH
16	27.2	CH_2	27.0	CH_2	37.4	CH_2	27.0	CH_2	37.1	CH_2
17	52.6	CH	52.4	CH	50.1	CH	51.9	CH	50.1	CH
18	11.7	CH_3	11.9	CH_3	12.8	CH_3	11.8	CH_3	12.7	CH_3
19	19.4	CH_3	18.9	CH_3	17.7	CH_3	15.0	CH_3	15.7	CH_3
20	39.0	CH	38.9	CH	39.0	CH	38.7	CH	38.6	CH
21	12.8	CH_3	12.8	CH_3	12.9	CH_3	12.5	CH_3	12.7	CH_3
22	65.1	CH	64.9	CH	69.8	CH	80.5	CH	64.8	CH
23	29.3	CH_2	29.4	CH_2	29.8	CH_2	31.7	CH_2	29.5	CH_2
24	65.3	C	65.1	C	62.8	C	76.0	C	64.8	C
25	63.9	C	63.9	C	61.4	C	72.5	C	63.8	C
26	91.8	CH	91.8	CH	101.6	CH	178.9	C	91.7	CH
27	16.6	CH_3	16.6	CH_3	14.8	CH_3	24.3	CH_3	16.6	CH_3
28	19.0	CH_3	19.0	CH_3	19.2	CH_3	23.1	CH_3	18.9	CH_3
OCH_3-3/26[b]					56.6	CH_3			56.8	CH_3
OAc-15[b]					170.7	C			170.8	C
					21.4	CH_3			21.4	CH_3

[a] Assignments of ^{13}C NMR data are based on DEPT, HMQC, and HMBC experiments.
[b] The number with the superscript indicates the location of the substituent group in the parent skeleton.

synthesis, the nitrite concentration was measured by the Griess reaction using the supernatant of the BV-2 cells. Briefly, 50 μL of the cell culture supernatant were reacted with 50 μL of Griess reagent [1:1 mixture of 0.1% *N*-(1-naphtyl)ethylenediamine in H_2O and 1% sulfanilamide in 5% phosphoric acid] in a 96 well plate and the absorbance was read with a microplate reader (Thermo Fisher Scientific Inc. America) at 550 nm. The experiments were performed in parallel three times, and the results are presented as the mean ± SD.

2.7. Molecular docking studies

Molecular docking simulations were performed using the software AutoDock Vina along with AutoDock Tools (ADT 1.5.6) using the hybrid Lamarckian Genetic Algorithm (LGA). The three dimensional (3D) crystal structure of iNOS (PDB code, 3E6T) was obtained from the RCSB Protein Data Bank, whose resolution was 2.5 Å [27]. The standard 3D structures (PDB format) of selected compounds for molecular docking were constructed by chem3D Pro 14.0 software, whose configurations were determined by their NOESY spectra and Chem3D modeling. The cubic grid box of 20 Å size (x, y, z) with a spacing of 1.000 Å and grid maps were built [28,29]. All of the other parameters were used according to default settings of AutoDock Vina. Results differing by less than 2.0 Å in positional root mean-square deviation (RMSD) were clustered together, and the results of the most favorable free energy of binding were chosen as the resultant complex structures.

3. Results and discussion

3.1. Structural elucidation

Compound **1** was obtained as an amorphous white powder. Its molecular formula was determined to be $C_{28}H_{44}O_5$, based on its ^{13}C NMR data and the HRESIMS $[M + H]^+$ ion at *m/z* 461.3270 (calcd for $C_{28}H_{45}O_5$, 461.3267). This molecular formula required seven unsaturation degrees. Its IR spectrum showed the presence of hydroxyl (3420 cm^{-1}) and olefinic (1646 cm^{-1}) functionalities. The ^1H NMR spectrum of **1** displayed signals for five aliphatic methyls [δ_H 0.69, 0.91 (d, J = 6.7 Hz), 1.03, 1.41, and 1.42], four oxymethine protons [δ_H 3.85 (1H, br s), 3.98 (1H, m), 3.73 (1H, dt, J = 10.7, 3.5 Hz), and 5.01 (1H, br s)], one olefinic proton [δ_H 5.59 (1H, br d, J = 5.4)], and some aliphatic methylene and methine protons in the high-field. The ^{13}C NMR spectrum of **1** revealed 28 carbon resonances, which included two olefinic carbons (δ_C 137.3 and 125.6), an acetal carbon (δ_C 91.8), and five oxygen-bearing carbons (δ_C 72.9, 66.4, 65.1, 65.3, and 63.9) (Table 1). These 28 skeletal carbons, especially the acetal carbon (δ_C 91.8), suggested that compound **1** possesses a withanolide-type skeleton according to those withanolides reported from the genus *Physalis* [30–34]. The following comprehensive analysis of 1D and 2D NMR data led to the construction of the rings A, B, C, D, and E. Correspondingly, the skeletal proton and carbon signals were assigned based on the HMQC, HMBC and ^1H–^1H COSY data. The olefinic, oxygenated, and acetal carbon signals (δ_C 137.3, 125.6, 72.9, 66.4, 65.1, 65.3, 63.9, and 91.8) were assigned to C-5, C-6, C-1, C-3, C-22, C-24, C-25, and C-26, respectively. The planar structure seemed to be established via the above NMR data analysis. However, the molecular formula based on this planar structure for compound **1** was not compatible with the HRESIMS data, suggesting the presence of another ring according to the index of hydrogen deficiency. According to the chemical shifts of C-24 (δ_C 65.3) and C-25 (δ_C 63.9) and HRESIMS data of compound **1**, a 24,25-epoxy structural moiety was proposed. Thus, the planar structure of **1** was finally determined as depicted in Fig. 1.

The configuration of compound **1** was deduced from the NOESY spectrum and Chem3D modeling, as well as TDDFT ECD calculations. NOESY interactions of H_3-19/H-1, H_3-19/H_3-18, H-1/H-2β, H-2α/H-3,

Table 2
^{1}H NMR data for compounds **1–5** (δ in ppm, J in Hz, 400 MHz, in $CDCl_3$).[a]

Position	1	2	3	4	5
1	3.85 br s	7.08 d (10.2)			
2α	2.09 m	6.31 dd (10.6,1.9)	6.20 d (9.9)	6.02 dd (10.0,2.5)	3.01 dd (15.0,6.2)
2β	1.75 m				2.62 br d (15.0)
3	3.98 m		6.93 dd (9.9,5.8)	6.85 ddd (10.0, 5.6,2.4)	3.71 s
4α	2.37 dd (13.3,3.9)	6.38 d (1.9)	3.76 d (5.8)	1.87 m	3.47 s
4β	2.29 t (11.8)			2.99 br d (18.8)	
6	5.59 br d (5.4)		3.23 br s	3.12 d (1.7)	3.20 s
7α	1.99 d (12.3)	2.69 dd (14.8,3.4)	2.05 m	2.03 m	2.11 m
7β	1.48 m	2.03 d (14.8)	1.52 m	1.34 m	1.51 m
8	1.45 m	1.57 m	1.71 m	1.55 m	1.60 m
9	1.56 td (11.3,5.3)	2.05 m	1.10 dt (11.9,4.7)	1.13 m	1.23 m
11α	1.46 m	1.73 m	1.43 m	1.49 m	1.38 m
11β	1.57 m	1.80 m	1.84 m	2.03 m	2.03 m
12α	1.20 m	1.25 m	1.21 m	1.17 m	1.19 m
12β	1.98 m	2.12 m	1.91 m	1.94 m	1.89 m
14	1.03 m	1.18 m	1.25 m	0.92 m	1.29 m
15α	1.13 m	1.12 m		1.13 m	
15β	1.62 m	1.64 m	4.81 dt (9.2,2.6)	1.62 m	4.80 t (9.0)
16α	1.38 m	1.36 m	1.53 m	1.38 m	1.51 m
16β	1.75 m	1.78 m	2.08 m	1.75 m	2.11 m
17	1.07 m	1.11 m	1.28 m	1.04 m	1.30 m
18	0.69 s	0.76 s	0.75 s	0.71 s	0.69 s
19	1.03 s	1.20 s	1.42 s	1.25 s	1.30 s
20	2.00 m	1.77 m	1.68 m	2.05 m	1.69 m
21	0.91 d (6.7)	0.92 d (6.70)	0.90 d (6.7)	0.97 d (6.7)	0.87 d (6.2)
22	3.73 dt (10.7,3.5)	3.71 dt (9.8,4.0)	3.54 dt (11.5,3.2)	4.77 dt (12.0,3.9)	3.62 m
23α	1.68 m	1.67 m	1.63 m	1.76 m	1.64 m
23β	1.31 m	1.31 m	1.83 m	1.95 m	1.32 m
26	5.01 br s	5.01 br s	4.57 br s		4.99 br s
27	1.42 s	1.43 s	1.31 s	1.41 s	1.41 s
28	1.41 s	1.41 s	1.35 s	1.32 s	1.41 s
OCH_3-3[b]					3.36 s
OAc-15[b]			2.03 s		2.04 s
OCH_3-26[b]			3.48 s		

[a] Assignments of ^{1}H NMR data are based on ^{1}H−^{1}H COSY, HMQC, and HMBC experiments.
[b] The number with the superscript indicates the location of the substituent group in the parent skeleton.

H_3-18/H-8, H-8/H-7β, H-9/H-7α, H-14/H-15α, H_3-18/H-20, H-22/H-17, H-22/H-23α, H-23β/H_3-28, H_3-26/H_3-27, and H_3-27/H_3-28, together with Chem3D modeling, implied a conformation for **1** as shown in Fig. 3, where the six-membered ring A existed in a boat conformation, rings B and C both existed in chair conformation, the five-membered ring D presented an envelope conformation, and ring E had a half-chair conformation. According to this molecular arrangement of **1**, rings B and C were deduced to be *trans*-fused with H-8 in a β-axial position and H-9 in an α-axial position, rings C and D were inferred to be *trans*-fused with H-14 in a α-axial position and Me-18 in a β-axial position, and the 24,25-epoxy moiety, relative to ring E, was on the α-face. Correspondingly, H-3, H-17, Me-21, and H-22 were all determined as α-oriented, H-1, Me-19, H-26, Me-27, Me-28 were all β-oriented. The absolute configuration of **1** was determined by the TDDFT ECD

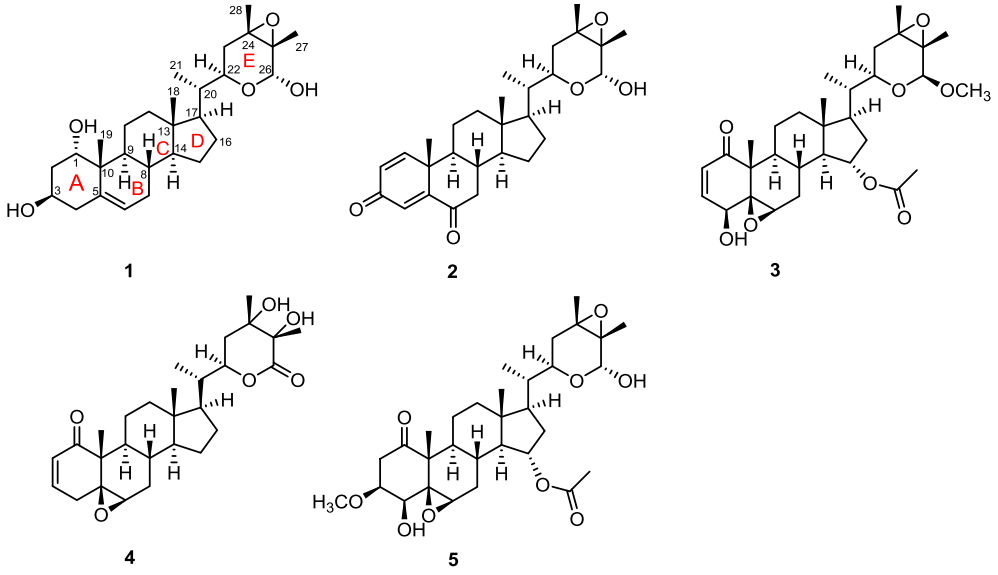

Fig. 1. Structures of compounds **1–5**.

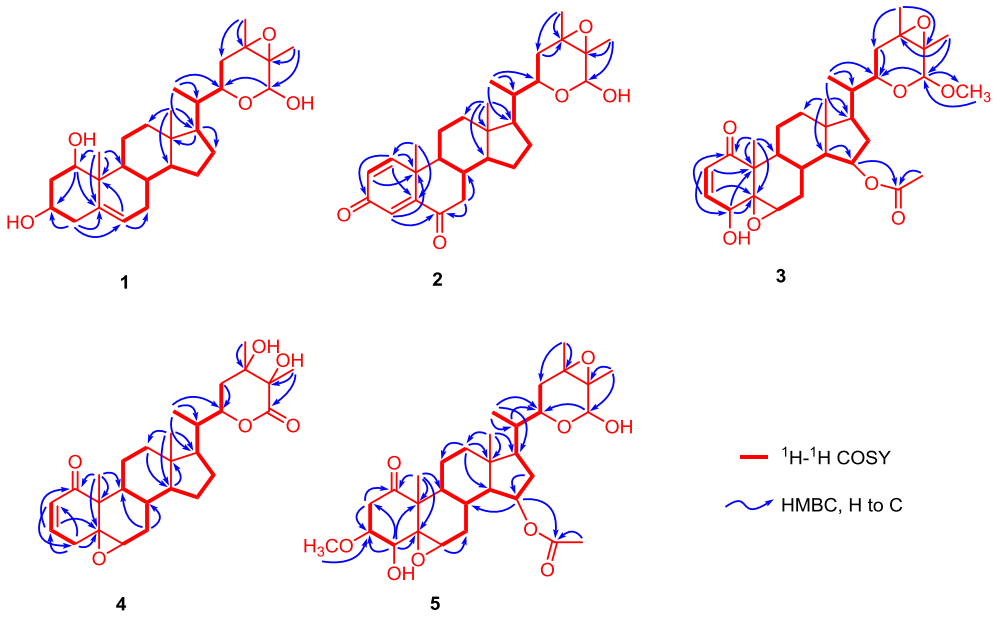

Fig. 2. ^{1}H – ^{1}H COSY and key HMBC correlations of compounds **1–5**.

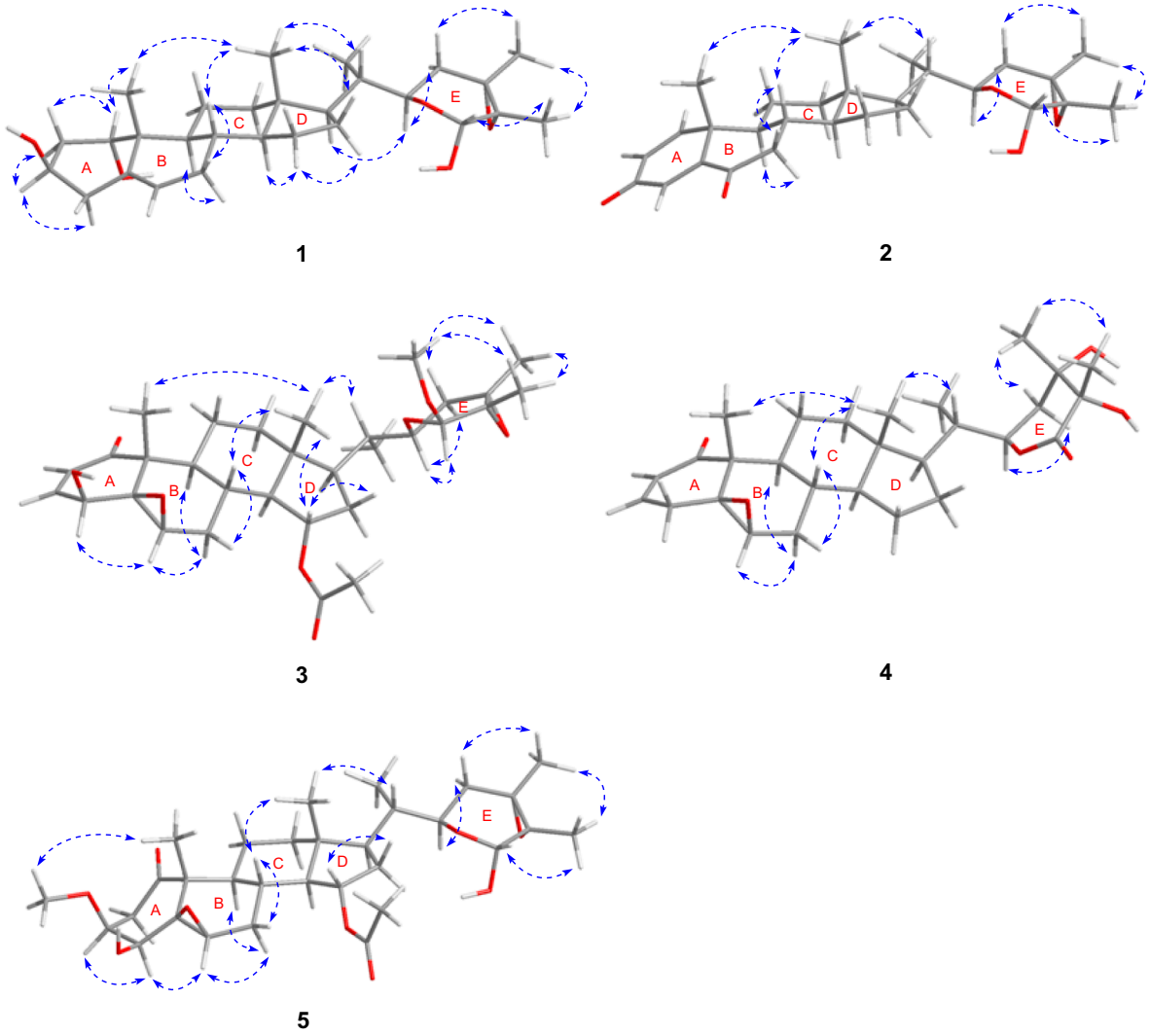

Fig. 3. Conformations and key NOESY correlations of compounds **1–5**.

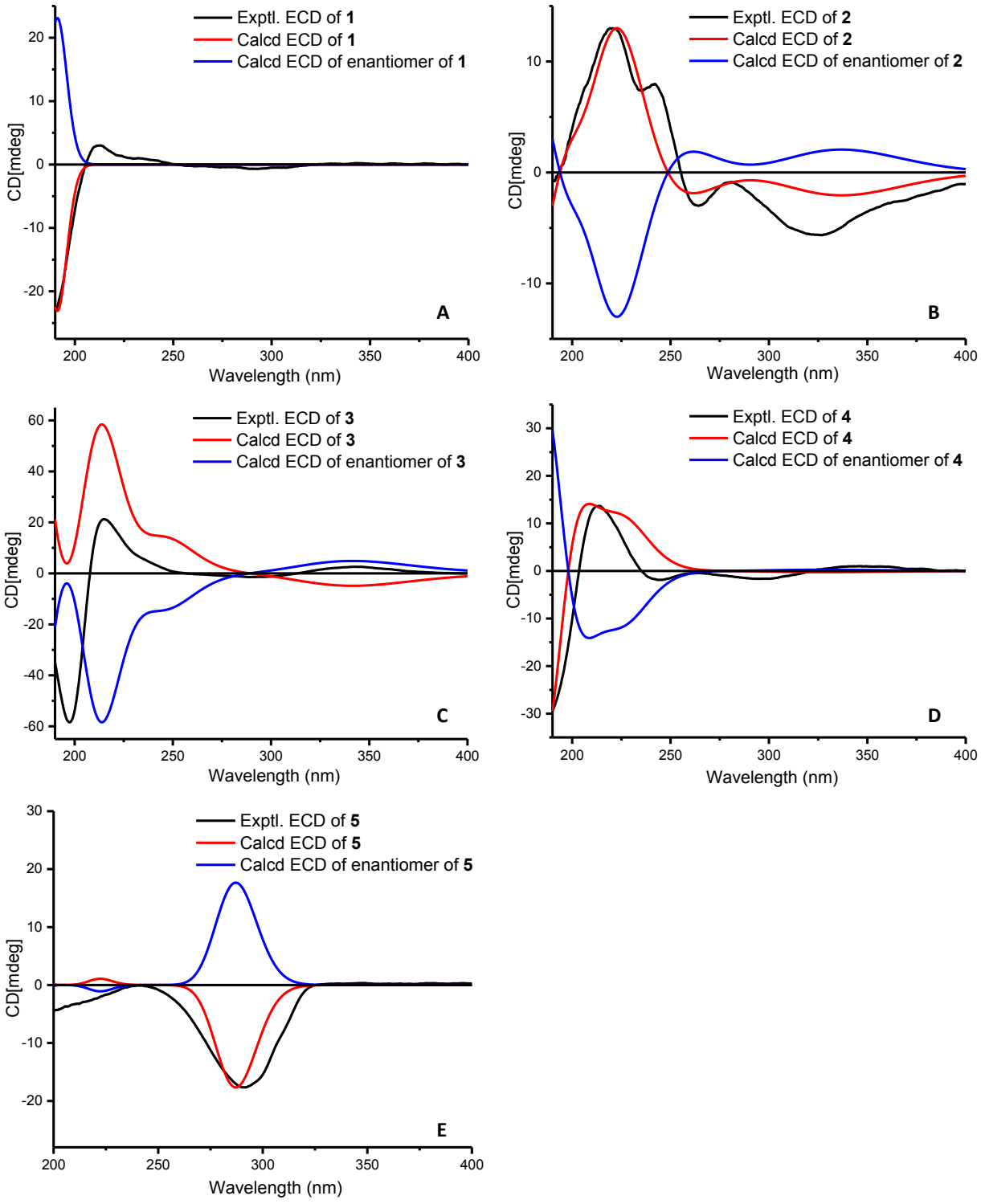

Fig. 4. Calculated and experimental ECD spectra of compounds **1**–**5** (A–E) in acetonitrile.

calculations, a powerful tool to determine the absolute configuration of natural products [11]. Starting from the conformation of **1** deduced from the NOESY correlations and Chem3D modeling, conformational searches with the MMFF94S force field by MOE software and geometry optimizations by the Gaussian 09 package were performed [24]. Then, the ECD calculations at the CAM-B3LYP/SVP level with the CPCM model were performed. The calculated ECD spectrum of **1** (Fig. 4A) is consistent with the experimental ECD spectrum, which suggested an absolute configuration of 1*S*, 3*R*, 8*S*, 9*S*, 10*R*, 13*S*, 14*S*, 17*R*, 20*S*, 22*R*, 24*S*, 25*S*, and 26*R*. On the basis of the above analysis, compound **1** was characterized unambiguously as shown in Fig. 1, and named peruvianolide A.

Compound **2**, isolated as a colorless solid, had a molecular formula of $C_{28}H_{38}O_5$ as shown by the HRESIMS $[M + H]^+$ ion at *m/z* 455.2800 (calcd for $C_{28}H_{39}O_5$, 455.2797) and the ^{13}C NMR data. The ^1H and ^{13}C NMR spectroscopic features of **2** were very similar to those of compound **1**, suggesting compound **2** is a withanolide related structurally to compound **1**. Analysis of its 1D and 2D NMR spectra revealed the

presence of the same rings C, D, and E as those of **1**. Apart from these resonances for the rings C, D, and E, the residual carbons at δ_C 153.6 (C-1), 128.1 (C-2), 185.4 (C-3), 125.0 (C-4), 161.5 (C-5), and 201.8 (C-6), together with the methylene [δ_C 46.9 (C-7)] and the quaternary carbon [δ_C 44.9 (C-10)], constituted rings A and B, of which ring B shared the C-8–C-9 unit with ring C. The further analysis of NMR spectra including ^{1}H–^{1}H COSY spectrum led to the accomplishment of the assignments of proton and carbon signals, and the planar structure was determined as shown in Fig. 2. As in the case of **1**, a NOESY experiment and Chem3D modeling were applied to elucidate the relative configuration of compound **2**. The NOESY correlations of H_3-19/H_3-18, H_3-18/H-8, H-7β/H-8, H-7α/H-9, H_3-18/H-20, together with Chem3D modeling, showed that the conformations of rings C, D, and E were the same as those of compound **1** and Me-19 was in a β-position (Fig. 3). As in the case of **1**, the experimental data matched the calculated ECD spectrum closely, suggesting a (8*S*,9*S*,10*R*,13*S*,14*S*,17*R*,20*S*,22*R*,24*S*,25*S*,26*R*) absolute configuration for **2**.

Compound **3** possessed a molecular formula of $C_{31}H_{44}O_8$ based on the HRESIMS (*m/z* 545.3119 $[M + H]^+$, calcd for $C_{31}H_{45}O_8$, 545.3114). Besides five similar methyls similar to those of compounds **1** and **2**, one acetyl methyl singlet (δ_H 2.03) and one methoxy group (δ_H 3.48) were observed from the ^{1}H NMR spectrum. In addition, four oxygenated methine protons, one suspected acetal proton (δ_H 4.57), and two olefinic protons (δ_H 6.20 and 6.93) were also displayed in its ^{1}H NMR spectrum. The ^{13}C NMR spectra exhibited 31 carbons, including the resonances for the methoxy group (δ_C 56.6) and acetyloxy group (δ_C 170.7 and 21.4). The remaining 28 carbons were indicative of a withanolide-type skeleton for compound **3**. Upon comparison of its ^{13}C NMR data with those of compounds **1** and **2**, the same rings C, D, and E were deduced, which were supported by the 2D NMR experiments. The remaining carbons constituted rings A and B as shown in Fig. 2 by analysis of the 1D and 2D NMR data, where the olefinic, ketone carbonyl, and three oxygenated carbons at δ_C 132.1, 142.0, 202.4, 69.6, 63.6, and 62.7 were assigned to C-2, C-3, C-1, C-4, C-5, and C-6, respectively. The methoxy group located at C-26 and the acetyloxy group attached at C-15 were determined from the HMBC correlations of H-26 to the methoxy carbon (δ_C 56.6) and the H-15 to the carbonyl carbon (δ_C 170.7). One more epoxy moiety, 5,6-epoxy was also proposed according to the chemical shift of C-5 (δ_C 63.6) and C-6 (δ_C 62.7) and the HRESIMS data. The NOESY data analysis indicated the whole molecular conformation of **3** were similar to those of compounds **1** and **2**, which showed the interactions of H_3-19/H_3-18, H_3-18/H-8, H_3-18/H-15, H-8/H-7β, H-4/H-6, H-6/H-7α, H-9/H-7α, H_3-18/H-20, H-22/H-26, H-22/H-23α, H_3-28/H-23β, and H_3-28/H_3-27 (Fig. 3). These correlations revealed the C-4 hydroxy group, the C-15 acetyloxy group, and the C-26 methoxy group were β-, α-, and β-oriented, and the 5,6-epoxy moiety was on the β-side. Using the same TDDFT calculations as applied for compounds **1** and **2**, the absolute configuration of **3** were deduced to be 4*S*, 5*R*, 6*R*, 8*R*, 9*S*, 10*R*, 13*R*, 14*S*, 15*S*, 17*R*, 20*S*, 22*R*, 24*S*, 25*S*, and 26*S* via comparison of experimental and calculated ECD spectra (Fig. 4C). Therefore, the structure of **3** was elucidated as shown in Fig. 1 and given a name peruvianolide C.

Compound **4** was obtained as an amorphous white powder. Its molecular formula was determined to be $C_{28}H_{40}O_6$ from the HRESIMS ion peak at *m/z* 473.2905 $[M + H]^+$ (calcd for $C_{28}H_{41}O_6$, 473.2903), which was consistent with its ^{13}C NMR data (Table 1). The ^{1}H and ^{13}C NMR data indicated compound **4** also to be a withanolide. Differing from those of compounds **1–3**, the acetal carbon (δ_C 91.8–101.6) disappeared in **4**, which was extrapolated to be replaced by a carbonyl carbon at (δ_C 178.9). Comparing the ^{13}C NMR data of compound **3** with those of **4**, the 24,25-epoxy moiety was inferred to be cleaved and two hydroxy groups were proposed according to the chemical shifts of C-24 (δ_C 76.0) and C-25 (δ_C 72.5) in **4**. The other skeletal characteristics different from those of compound **3** are that there is no acetyl group present in **4** and two less oxygenated carbons were observed in the ^{13}C NMR spectrum of **4**. Analysis of its 1D and 2D NMR data revealed that the oxygenated carbons C-4 (δ_C 69.6) and C-15 (δ_C 76.0) in **3** were deoxidized to form two methylenes in compound **4**. The assignments of all the protons and carbons were accomplished by detailed analysis of 2D NMR spectra. The NOESY spectrum of **4** indicated a similar conformation to that of **3**, where the hydroxy groups located at C-24 and C-25 were determined as both α-oriented. Using the same calculation method as for compounds **1–3**, the calculated ECD spectrum of **4** was obtained, which accorded with the experimental ECD data closely. Thus, a (5*S*,6*R*,8*S*,9*S*,10*R*,13*S*,14*S*,17*R*,20*S*, 22*R*,24*S*,25*S*) absolute configuration for **4** was established and the compound was named peruvianolide D.

Compound **5** gave a molecular formula of $C_{31}H_{46}O_9$ as deduced from the HRESIMS ion peak at *m/z* 585.3037 $[M + Na]^+$ (calcd for $C_{31}H_{46}NaO_9$, 585.3040) and the ^{13}C NMR data. The ^{1}H and ^{13}C NMR spectra revealed compound **5** should be a withanolide carrying a methoxy (δ_C 56.8; δ_H 3.36) and an acetyloxy group (δ_C 170.8 and 21.4; δ_H 2.04). By comparison of its ^{13}C NMR data with those of compound **3**, the olefinic carbons disappeared and one more oxygenated carbon was observed in **5**. The following 2D NMR experiments were performed, which led to the establishment of structure of compound **5**, where the oxygenated, acetal, and carbonyl carbons at δ_C 77.5, 74.9, 91.7, and 209.8 were assigned to C-3, C-4, C-26, and C-1, respectively. The HMBC couplings of H-3 with the methoxy carbon (δ_C 56.8) and H-15 with the carbonyl carbon (δ_C 170.8), revealed that the methoxy group was attached at C-3 and the acetyoxy group was at C-15. The NOESY spectrum showed the proton interactions of H-3/H-4, H-4/H-6, H-6/H-7α, H-8/H-7β, H-9/H-7α, H_3-18/H-8, H_3-18/H-20, H-15/H-16β. These NOE effects showed the molecular conformation of **5** was similar to those of compounds **1–4**. In this arrangement of **5**, the C-3 methoxy group, the hydroxy groups located at C-4 and C-26, the C-15 acetyloxy group, and the 5,6-epoxy and 24,25-epoxy moieties were assigned as β-, β-, α-, α-, β-, and α-oriented, respectively. Similarly, using the TDDFT calculations, the absolute configuration of **5** was deduced to be 3*S*, 4*S*, 5*R*, 6*R*, 8*R*, 9*S*, 10*R*, 13*R*, 14*S*, 15*S*, 17*R*, 20*S*, 22*R*, 24*S*, 25*S*, and 26*R*, by comparing the experimental data with those calculated by the TDDFT method (Fig. 4E), Accordingly, the planar structure of **5** was assigned as depicted in Fig. 1 and named peruvianolide E.

3.2. NO inhibitory activities

NO is an important signaling molecule that has a close relationship with inflammation. Compounds inhibiting NO production may be developed into potential lead compounds for the treatment of neuroinflammation and related neurodegenerative diseases [9]. Compounds **1–5** isolated from *P. peruviana* were tested for their NO inhibitory effects according to the method described previously [11,35]. The NO inhibitor, 2-methyl-2-thiopseudourea, sulfate (SMT), was used as control. (IC_{50} value, 2.40 μM) [36]. All the isolates suppressed NO generation induced by LPS in murine microglial BV-2 cells and the IC_{50} values were shown in Table 3. According to their IC_{50} values, compounds **2–4** showed strong inhibitory effects on NO production,

Table 3
IC_{50} values of compounds **1–5** inhibiting NO production in BV-2 cells.

Compound	IC_{50} (μM)[a]
1	> 10
2	7.0 ± 0.2
3	1.5 ± 0.1
4	1.4 ± 0.1
5	> 60
SMT[a]	2.4 ± 0.2

[a] SMT(2-methyl-2-thiopseudourea, sulfate) was used as a positive control. Data are presented based on three experiments.

Table 4
Logarithms of free binding energies (FBE, kcal/mol) of NO inhibitors to the active cavities of iNOS (PDB code: 3E6T) and targeting residues of the binding site located on the mobile flap.

Compound	−Log (FBE)	Targeting residues
2	−10.6	TYR-367
3	−10.2	ARG-375 GLN-257 ALA-345
4	−10.4	ARG-260 ALA-276 SER-256

especially compounds **3** and **4** exhibited stronger activities compared to positive control. The cytotoxic test (MTT assay) showed that all of the isolates had no impact on BV-2 cell survival at their effective concentrations for the inhibition of NO production (data not shown).

3.3. Interactions of bioactive compounds with the iNOS protein

NO production is regulated by three types of nitric oxide synthase (NOS): endothelial NOS (eNOS), neural NOS (nNOS), and inducible NOS (iNOS), of which iNOS is critical and in charge of the amount of NO in inflammatory process [37]. To investigate the possible mechanism of inhibitory effects, molecular docking studies were performed to explore the interactions of the bioactive compounds with the iNOS protein [27,38]. The bioactive compounds **2–4** (IC_{50} value < 8 μM) were selected for the docking studies and results indicated that compounds **2–4** have strong interactions with the iNOS protein. The logarithms of free binding energies and the binding residues are shown in Table 4. According to the results of molecular docking, compounds **2–4** with strong NO inhibitory effects showed strong binding affinities with the iNOS protein, implying the possible mechanism of NO inhibition of these bioactive compounds is to interact with the iNOS protein by targeting residues of the active cavities of iNOS protein (Fig. 5).

4. Conclusion

The results herein provide phytochemical and biological data concerning the withanolides isolated from *P. peruviana*. Five previously unreported withanolides (**1–5**) have been isolated. Their structures were elucidated on the basis of extensive 1D and 2D NMR spectroscopic data analysis, and the absolute configurations were established by comparing their experimental CD spectra with those calculated by the TDDFT method. In addition, biological evaluation showed that compounds **2–4** exerted more NO inhibitory effects with IC_{50} values below 8 μM. Molecular docking revealed that compounds **2–4** had strong interactions with the iNOS protein by targeting residues of the active cavities of iNOS, disclosing that the possible mechanism of bioactive compounds to inhibit NO production. These results indicated that the plant *P. peruviana* has potential medicinal value for medical inflammatory diseases. While, the more bioactive compounds **2–4** may have the potential to be developed as anti-inflammatory agents for various inflammatory diseases and other related disorders.

Conflict of interest

The authors of the present manuscript have declared that no competing interests exist.

Acknowledgments

This research was financially supported by the National Natural Science Foundation of China (Nos. U1703107, 21642016, and 21372125), the National Key Research and Development Program of China (No. 2018YFA0507204), the Natural Science Foundation of Tianjin, China (No. 16JCYBJC27700), the Hundred Young Academic Leaders Program of Nankai University, and State Key Laboratory for Chemistry and Molecular Engineering of Medicinal Resources (Guangxi Normal University, No. CMEMR2018-B02).

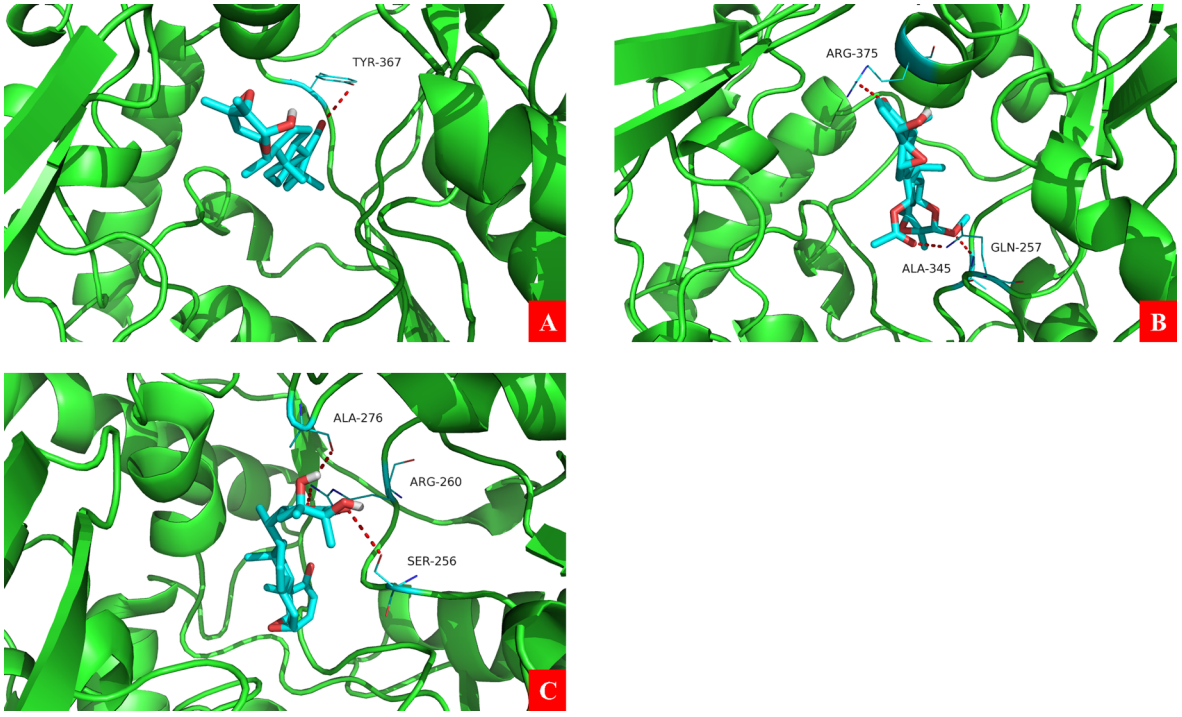

Fig. 5. Molecular docking simulations obtained at the lowest energy conformation, highlighting potential hydrogen contacts of compounds **2–4** (A–C), respectively. (Colored by atom: carbon is cyan; nitrogen is blue; oxygen is red; hydrogen is gray; sulfur is orange). For clarity, only interacting residues are labeled. Hydrogen bonding interactions are shown by dashes. These figures were created by PyMOL.

Appendix A. Supplementary material

Supplementary data to this article can be found online at https://doi.org/10.1016/j.bioorg.2019.03.051.

References

[1] D.S. Bredt, S.H. Snyder, Annu. Rev. Biochem. 63 (1994) 175–195.
[2] T.J. Guzik, R. Korbut, T. Adamek-Guzik, J. Physiol. Pharmacol. 54 (2003) 469–487.
[3] A. Contestabile, Brain Res. Rev. 32 (2000) 476–509.
[4] C.Q. Li, B. Pang, T. Kiziltepe, L.J. Trudel, B.P. Engelward, P.C. Dedon, G.N. Wogan, Chem. Res. Toxicol. 19 (2006) 399–406.
[5] M.P. Pando, I.M. Verma, J. Biol. Chem. 275 (2000) 21278–21286.
[6] B. Liu, H.M. Gao, J.Y. Wang, G.H. Jeohn, C.L. Cooper, J.S. Hong, Ann. N. Y. Acad. Sci. 962 (2002) 318–331.
[7] A. Fernandes, L. Miller-Fleming, Cell. Mol. Life Sci. 71 (2014) 3969–3985.
[8] P. Grammas, J. Neuroinflammation 8 (2011) 1–12.
[9] S. Shadfar, C.J. Hwang, M.S. Lim, D.Y. Choi, J.T. Hong, Arch. Pharm. Res. 38 (2015) 2106–2119.
[10] J. Xu, X. Sun, J. Kang, F. Liu, P. Wang, J. Ma, H. Zhou, D.Q. Jin, Y. Ohizumi, D. Lee, M. Bartlam, Y. Guo, J. Funct. Foods 32 (2017) 37–45.
[11] P. Wang, X. Yang, F. Liu, Y. Liang, G. Su, M. Tuerhong, D.Q. Jin, J. Xu, D. Lee, Y. Ohizumi, Y. Guo, Bioorg. Chem. 76 (2018) 53–60.
[12] Editorial Committee of the Flora of China, Flora Reipublicae Popularis Sinicae, Vol. 67 (1) (1978) 59.
[13] Nanjing University of Chinese Medicine, Dictionary of Chinese Materia Medica, 2nd ed., Shanghai Scientific and Technological Press, Shanghai, 2006, pp. 1347 – 1348.
[14] Y.M. Xu, E.M.K. Wijeratne, A.L. Babyak, H.R. Marks, A.D. Brooks, P. Tewary, L.J. Xuan, W.Q. Wang, T.J. Sayers, A.A.L. Gunatilaka, J. Nat. Prod. 80 (2017) 1981–1991.
[15] M. Sang-ngern, U.J. Youn, E.J. Park, T.P. Kondratyuk, C.J. Simmons, M.M. Wall, M. Ruf, S.E. Lorch, E. Leong, J.M. Pezzuto, L.C. Chang, Bioorg. Med. Chem. Lett. 26 (2016) 2755–2759.
[16] L.N. Dinan, S.D. Sarker, V. Šik, Phytochemistry 44 (1997) 509–512.
[17] S.T. Fang, J.K. Liu, B. Li, J. Asian Nat. Prod. Res. 12 (2010) 618–622.
[18] Y.H. Lan, F.R. Chang, M.J. Pan, C.C. Wu, S.J. Wu, S.L. Chen, S.S. Wang, M.J. Wu, Y.C. Wu, Food Chem. 116 (2009) 462–469.
[19] S.T. Fang, J.K. Liu, B. Li, Steroids 77 (2012) 36–44.
[20] S. Ahmada, A. Malika, R. Yasmin, N. Ullah, W. Gul, P.M. Khan, H.R. Nawaz, N. Afza, Phytochemistry 50 (1999) 647–651.
[21] A. Saeed, Y. Rehana, M. Abdul, Chem. Pharm. Bull. 47 (1999) 477–480.
[22] S. Kensuke, I. Hiroshi, K. Shinobu, I. Toru, Chem. Pharm. Bull. 24 (1976) 1403–1405.
[23] L.X. Chen, H. He, F. Qiu, Nat. Prod. Rep. 28 (2011) 705–740.
[24] M.J. Frisch, G.W. Trucks, H.B. Schlegel, G.E. Scuseria, M.A. Robb, J.R. Cheeseman, G. Scalmani, V. Barone, B. Mennucci, G.A. Petersson, H. Nakatsuji, M. Caricato, X. Li, H.P. Hratchian, A.F. Izmaylov, J. Bloino, G. Zheng, J.L. Sonnenberg, M. Hada, M. Ehara, K. Toyota, R. Fukuda, J. Hasegawa, M. Ishida, T. Nakajima, Y. Honda, O. Kitao, H. Nakai, T. Vreven, J.A. Montgomery Jr., J.E. Peralta, F. Ogliaro, M. Bearpark, J.J. Heyd, E. Brothers, K.N. Kudin, V.N. Staroverov, R. Kobayashi, J. Normand, K. Raghavachari, A. Rendell, J.C. Burant, S.S. Iyengar, J. Tomasi, M. Cossi, N. Rega, J.M. Millam, M. Klene, J.E. Knox, J.B. Cross, V. Bakken, C. Adamo, J. Jaramillo, R. Gomperts, R.E. Stratmann, O. Yazyev, A.J. Austin, R. Cammi, C. Pomelli, J.W. Ochterski, R.L. Martin, K. Morokuma, V.G. Zakrzewski, G.A. Voth, P. Salvador, J.J. Dannenberg, S. Dapprich, A.D. Daniels, O. Farkas, J.B. Foresman, J.V. Ortiz, J. Cioslowski, D.J. Fox, Gaussian 09, Revision D.01, Gaussian, Inc., Wallingford CT, 2009.
[25] T. Bruhn, A. Schaumlöffel, Y. Hemberger, G. Bringmann, SpecDis, Version 1.62, University of Wuerzburg, Germany, 2014.
[26] T. Mosmann, J. Immunol. Meth. 65 (1983) 55–63.
[27] E.D. Garcin, A.S. Arvai, R.J. Rosenfeld, M.D. Kroeger, B.R. Crane, G. Andersson, G. Andrews, P.J. Hamley, P.R. Mallinder, D.J. Nicholls, S.A. St-Gallay, A.C. Tinker, N.P. Gensmantel, A. Mete, D.R. Cheshire, S. Connolly, D.J. Stuehr, A. Aberg, A.V. Wallace, J.A. Tainer, E.D. Getzoff, Nat. Chem. Biol. 4 (2008) 700–707.
[28] M.A. Loza-Mejía, J.R. Salazar, J. Mol. Graph. Model. 62 (2015) 18–25.
[29] R. Gautam, S.M. Jachak, V. Kumar, C.G. Mohan, Bioorg. Med. Chem. Lett. 21 (2011) 1612–1616.
[30] G.Y. Xia, T. Yao, B.Y. Zhang, T. Li, N. Kang, S.J. Cao, L.Q. Ding, L.X. Chen, F. Qiu, Org. Biomol. Chem. 15 (2017) 10016–10023.
[31] C.M. Cao, H. Zhang, R.J. Gallagher, V.W. Day, K. Kindscher, P. Grogan, M.S. Cohen, B.N. Timmermann, J. Nat. Prod. 77 (2014) 631–639.
[32] L.X. Chen, G.Y. Xia, H. He, J. Huang, F. Qiu, X.L. Zi, RSC ADV. 6 (2016) 52925–52936.
[33] G. Xia, Y. Li, J. Sun, L. Wang, X. Tang, B. Lin, N. Kang, J. Huang, L. Chen, F. Qiu, Steroids 115 (2016) 136–146.
[34] L. Ji, Y. Yuan, Z. Ma, Z. Chen, L. Gan, X. Ma, Steroids 78 (2013) 860–865.
[35] W.S. Suh, K.J. Park, D.H. Kim, L. Subedi, S.Y. Kim, S.U. Choi, K.R. Lee, Bioorg. Chem. 72 (2017) 156–160.
[36] J. Ma, X. Yang, P. Wang, B. Dong, G. Su, M. Tuerhong, D.Q. Jin, J. Xu, D. Lee, Y. Ohizumi, J. Lin, Y. Guo, Bioorg. Chem. 75 (2017) 71–77.
[37] S.R. Lee, S. Lee, E. Moon, H.J. Park, H.B. Park, K.H. Kim, Bioorg. Chem. 70 (2017) 94–99.
[38] Z. Shi, L. An, X. Yang, Y. Xi, C. Zhang, Y. Shuo, J. Zhang, D.Q. Jin, Y. Ohizumi, D. Lee, J. Xu, Y. Guo, Bioorg. Chem. 84 (2019) 177–185.